Available online at www.sciencedirect.com
SCIENCE DIRECT®
Catalysis Today 86 (2003) 17–29
CATALYSIS TODAY
www.elsevier.com/locate/cattod

Morphology and orientation of MoS_2 clusters on Al_2O_3 and TiO_2 supports and their effect on catalytic performance

Hiromichi Shimada*

National Institute of Advanced Industrial Science and Technology (AIST), 1-1 Higashi, Tsukuba, Ibaraki 305-8561, Japan

Received 14 March 2003; received in revised form 14 May 2003; accepted 19 May 2003

Abstract

The catalytic performance of MoS_2-based hydrotreating catalysts strongly depends on their morphology and orientation on the support. The effects of the morphology and orientation of MoS_2 clusters on supports, typically Al_2O_3 and TiO_2, on the catalytic performance are reviewed here, focusing on recently reported epitaxial relationships at the interface between MoS_2 clusters and the support.

Keywords: MoS_2; Orientation; Epitaxial; TEM; HDS

1. Introduction

Regulations for diesel fuel quality in the near future require improvements in the catalytic performances of *hydrodesulfurization* (HDS) catalysts. For example, HDS catalysts will be required to remove sulfur from *hard-to-desulfurize* compounds, such as 4,6-dimethyldibenzothiophene, by eliminating the steric hindrance [1–3]. For MoS_2-based HDS catalysts, maximum dispersion of their active catalytic sites is essential to satisfy this requirement, and detailed knowledge of the relationships between the catalytic structures and activities is needed.

Studies on the structure–activity relationships reveal that the so-called "Co(Ni)–Mo–S" structure proposed by Topsøe et al. [4] in the late 1980s is now widely accepted as the structural model for the active center of MoS_2-based binary sulfide catalysts. A recent review [5], however, states that only a part of the Co–Mo–S structure likely functions as highly active catalytic sites in industrial catalysts. Thus, further investigation into the microstructure of MoS_2-based HDS catalysts and its relevance to the catalytic performance is needed to determine the most active structure of binary sulfide catalyst systems.

Candia et al. [6] claimed that there are at least two kinds of Co–Mo–S structures; "Co–Mo–S(I)", which has strong electronic interaction with the support, and "Co–Mo–S(II)", which has weak interaction with the support. Co–Mo–S(I) is less catalytically active than Co–Mo–S(II). Studies [7–12] indicate that single-layered MoS_2 clusters with Co at their edges are Co–Mo–S(I), whereas multi-layered MoS_2 clusters with Co, except the bottom layer, are Co–Mo–S(II). Furthermore, Whitehurst et al. [13] reported an effect of steric hindrance by which the bottom layer of Co–Mo–S structure is less active than the other layers. These reports showed that the catalytic activity of Co–Mo–S structures depends on the morphology of the MoS_2 clusters on the support and that MoS_2 clusters with high aspect ratios (cluster thickness,

* Tel.: +81-298-61-9012; fax: +81-298-61-2371.
E-mail address: h-shimada@aist.go.jp (H. Shimada).

0920-5861/$ – see front matter © 2003 Elsevier B.V. All rights reserved.
doi:10.1016/S0920-5861(03)00401-2

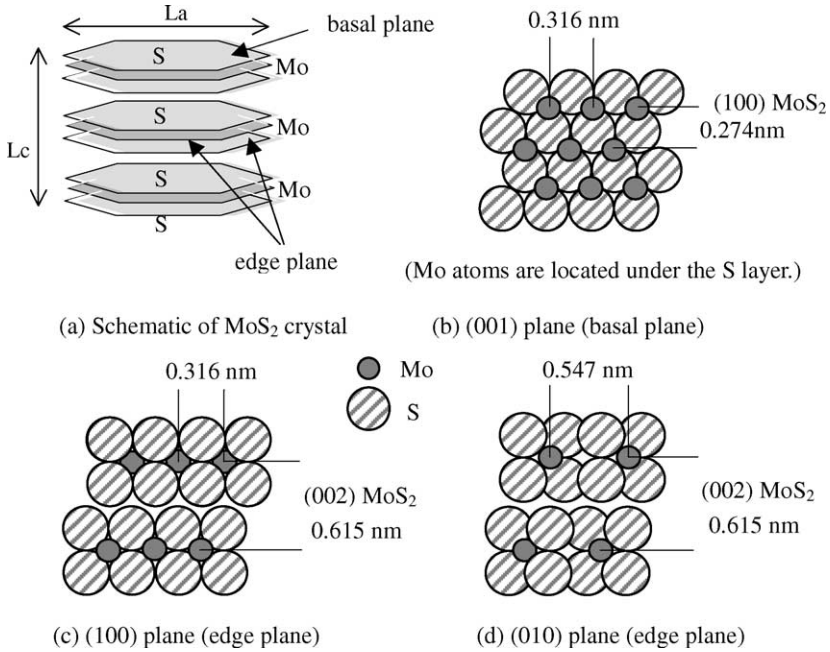

Fig. 1. Crystal structure of MoS_2: (a) overall structure, (b) (0 0 1) plane, (c) (1 0 0) plane, and (d) (1 1 0) plane.

L_c, divided by cluster lateral dimension, L_a) possess higher intrinsic activities than those with low aspect ratios (Fig. 1a). These results clearly indicate that all the edge planes of MoS_2 are not equal from the viewpoint of catalytic activity of binary sulfide catalysts, although all the discussions in those studies assumed that active catalytic sites of MoS_2 are only at the edge planes, (1 0 0) planes, and (1 1 0) planes (Fig. 1b–d).

Several studies indicate that the morphology of MoS_2 clusters also affects the catalytic activities of MoS_2 catalysts without Co- or Ni-promoters. For example, Nishijima et al. [14] proposed that multilayered MoS_2 clusters on an Al_2O_3 support are hydrogenolysis-oriented, whereas single-layered MoS_2 clusters on an Al_2O_3 support are hydrogenation (HYD)-oriented (Fig. 2). Vrinat et al. [15] reported that only the topmost layers of MoS_2 clusters on the support are catalytically active in the HDS reaction of thiophene. Massoth and Muralidhar [16] concluded that only the corner sites of MoS_2 clusters on an Al_2O_3 support (Fig. 3) are catalytically active for HDS, whereas all the edge planes of the clusters are active for HYD. Based on a geometrical model of unsupported MoS_2 catalysts, Kasztelan et al. [17] concluded that both HDS and HYD reactions are catalyzed on the edge planes. Daage and Chianelli [18] proposed the *rim-edge model* (Fig. 3) in which HYD of dibenzothiophene (DBT) to tetrahydrodibenzothiphene is catalyzed exclusively on the top and bottom of edge planes (called *rim sites*) and direct sulfur-extrusion to biphenyl is catalyzed on all the edge planes of unsupported MoS_2 catalysts (Fig. 3). These results indicate that the morphology of MoS_2 clusters, in particular the aspect ratio (L_c/L_a, Figs. 1

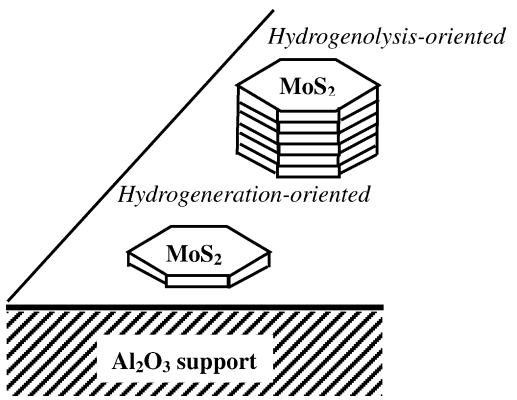

Fig. 2. MoS_2 catalysts with HYD-oriented and hydrogenolysis-oriented structures (original concept was shown in [14]).

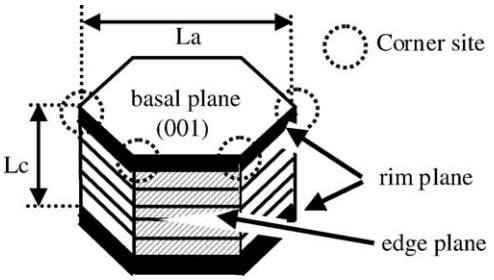

Fig. 3. Rim-edge model of MoS_2 catalysts (original concept was shown in [18]).

and 3), affects the catalytic performance, irrespective of the presence or absence of Co- or Ni-promoters. In addition, both the electronic interaction between MoS_2 clusters and the support and the steric hindrance should be considered causes of the effects of the cluster morphology on the catalytic performance.

These above-mentioned results on the effect of the morphology of MoS_2 clusters on the catalytic activity assumed that layered MoS_2 clusters (Figs. 1a and 2) lie on the support surface via so-called "basal bonding" in which basal planes ((0 0 1) plane, Fig. 1b) of MoS_2 crystals are attached to the surface of the catalyst support (Fig. 2). In addition to the basal bonding, however, "edge bonding" is also evident, in which edge planes ((1 0 0) or (1 1 0) plane, Fig. 1c and d) of MoS_2 crystals are attached to the support surface. Thus, catalytic activity of Co–Mo–S structures depends not only on the morphology but also on the orientation of MoS_2 clusters on the support, because the upper edge sites of the edge-bonded MoS_2 clusters that are perpendicular to the support surface (Fig. 4a) supposedly have weaker electronic interaction with the support than do single-layered MoS_2 clusters that are basal-bonded to the support (Fig. 4b) [10]. In addition, the upper edge sites of the edge-bonded MoS_2 clusters have less steric hindrance than do either the edge sites of the basal-bonded single-layered MoS_2 clusters (Fig. 4b) or edge sites of the bottom layers of the basal-bonded multi-layered MoS_2 clusters (Fig. 4c).

Until recently, no clear evidence has been reported for such edge-bonded MoS_2 clusters on supports, although the orientation of the MoS_2 clusters has been investigated by using transmission electron spectroscopic (TEM) observations [19–22]. Recently, using single-crystal model catalyst systems, Sakashita et al. [23–25] obtained evidence for edge-bonded MoS_2 clusters on a single-crystal face of γ-Al_2O_3 surface. Subsequent studies [26,27] confirmed the relationship between the morphology and orientation of MoS_2 clusters and the surface structure of γ-Al_2O_3 powder supports, and showed that the catalytic activity and selectivity depend on the cluster morphology on the support [27]. The presence of edge-bonded MoS_2

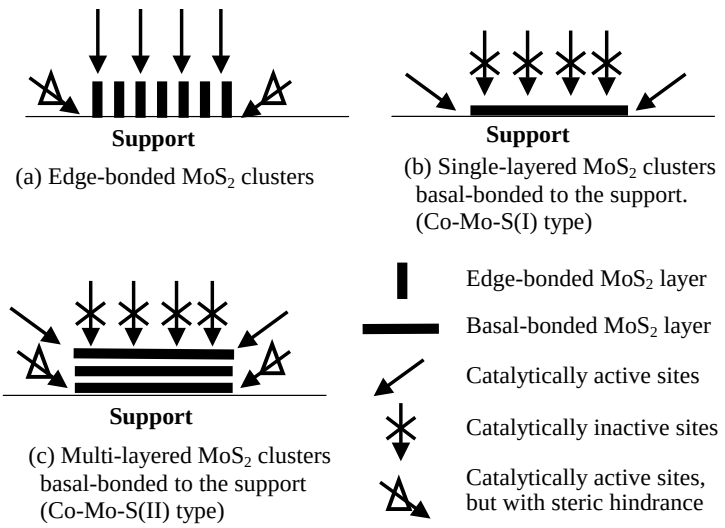

Fig. 4. Morphology and orientation of MoS_2 clusters on supports: (a) edge-bonded MoS_2 cluster, (b) single-layered MoS_2 cluster basal-bonded to the support, and (c) multi-layered MoS_2 cluster basal-bonded to the support (original concept was shown in [29]).

clusters was confirmed on anatase-type TiO_2 supports as well as on γ-Al_2O_3 surface supports [28]. A subsequent study [29] reported the catalytic properties of edge-bonded MoS_2 clusters on TiO_2 and compared them with those of basal-bonded MoS_2 clusters on the same support. The present review discusses recent studies on the morphology and orientation of MoS_2 clusters on γ-Al_2O_3 and TiO_2 supports, focusing on the above-mentioned series of studies [23–29].

2. Morphology and orientation of MoS_2 clusters on γ-Al_2O_3 single-crystal surface

Pratt et al. [19] investigated the orientation of MoS_2 clusters (by using TEM observations) and reported that the clusters were standing upright as flakes (up to five layers) on γ-Al_2O_3 powders with edge bonding. However, Srinivasan et al. [20] argued with this conclusion and insisted that distinguishing between edge-bonded and basal-bonded MoS_2 clusters is difficult due to the porous structure of conventional γ-Al_2O_3 powders. They concluded that no MoS_2 clusters were edge-bonded to catalyst supports such as Al_2O_3, TiO_2 and SiO_2. To overcome the problem of a porous support, Hayden and Dumesic [21] used a flat γ-Al_2O_3 surface as the catalyst support and reported the presence of hexagonally shaped MoS_2 clusters with edge bonding to the surface. Stockmann et al. [22] attributed the conclusions by Hayden and Dumesic [21] to the presence of microporous structures that lead to misinterpretation between edge-bonded and basal-bonded MoS_2 clusters and rather concluded that all the MoS_2 clusters were basal-bonded to the γ-Al_2O_3 surface. As mentioned in Section 1, TEM observations have not yet provided conclusive evidence for edge-boded MoS_2 clusters on γ-Al_2O_3 supports, although the basal-bonded structures have been widely accepted since Schuit and Gates [30] first proposed a "*monolayer model*" for the active catalytic sites of the Co–Mo–S structure.

Model catalyst systems using metal oxide thin films [21,31–35] evidently have an advantage over conventional powder supports in the determination of the morphology and orientation of MoS_2 clusters. As pointed out by Stockmann et al. [22], the use of flat oxide surfaces without porous structures is needed to conclusively determine the orientation of MoS_2 clusters on the catalyst support. Furthermore, polycrystalline surface structures of the support would give ambiguous conclusions, because the formation of uniform structures of MoS_2 clusters would be hindered.

Based on this background, Sakashita et al. [23–25] used γ-Al_2O_3 *single-crystal* surfaces as the model supports of MoS_2 catalysts. They fabricated γ-Al_2O_3 single crystals as thin films on spinel ($MgAl_2O_4$) single-crystal substrates with surface orientation of (1 1 1) and (1 0 0), because obtaining large γ-Al_2O_3 bulk single crystals is difficult [23]. After flat (1 1 1) and (1 0 0) planes of γ-Al_2O_3 surface were confirmed, Sakashita et al. prepared MoS_2 model catalysts by vacuum evaporation of MoO_x on the substrates, followed by sulfidation using 5% H_2S/H_2. Fig. 5a shows a TEM photograph of the observed MoS_2 clusters on (1 1 1) γ-Al_2O_3 [23]. The photograph shows lattice images of the MoS_2 clusters with a spacing of 0.25 nm crossed $(2\,0\,\bar{2})$ γ-Al_2O_3 at an angle of 30°. This was interpreted as the schematic diagram shown in Fig. 5b of the interface between γ-Al_2O_3 and MoS_2 clusters, where Mo atoms replaced Al atoms in the octahedral cation positions in the same way as the so-called B-layer [30,36] of γ-Al_2O_3. The observed interplanar spacing (0.25 nm) of MoS_2 clusters was assigned to (1 0 0) MoS_2. The Mo–Mo distance of 0.316 nm corresponded to the Al–Al distance of 0.28 nm with a lattice misfit of 11%. Epitaxial relationship was (0 0 1) MoS_2//(1 1 1) γ-Al_2O_3 with [1 1 0] MoS_2//[1 0 1] γ-Al_2O_3.

The TEM photograph of MoS_2 clusters on (1 0 0) γ-Al_2O_3 (Fig. 6a) shows numerous short black lines assigned to MoS_2 clusters [23]. Although most of the lines were "single" straight or curved lines, some of the straight lines yield a lattice image with a spacing of about 0.6 nm. This spacing was assigned to the interplanar spacing of (0 0 2) MoS_2 (0.615 nm), and thus the lattice image was identified as edge-bonded MoS_2 clusters observed from the [0 0 1] direction. The interface structure was assumed as shown in Fig. 6b, where the Mo–Mo distance along the *c*-axis (0.615 nm) corresponded to twice the Al–Al distance (0.28 nm) with 9% contraction and the Mo–Mo distance perpendicular to the *c*-axis (0.547 nm) corresponded to twice the Al–Al distance (0.28 nm) with 3% elongation. Epitaxial relationship was (1 1 0) MoS_2//(1 0 0) γ-Al_2O_3 with [0 0 1] MoS_2//[0 1 1] γ-Al_2O_3. The above misfits

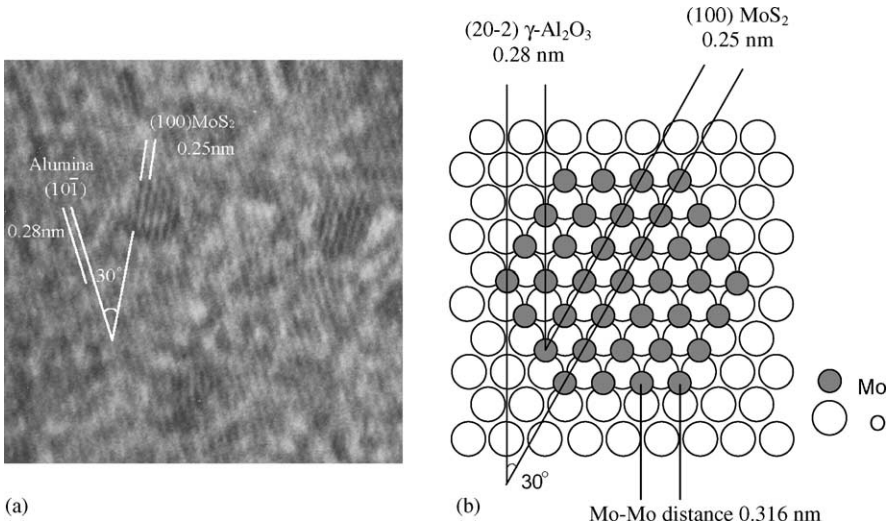

Fig. 5. (a) TEM photograph of MoS_2 clusters supported on (1 1 1) γ-Al_2O_3/$MgAl_2O_4$ substrate after sulfidation at 773 K and (b) schematic diagram of interface between MoS_2 clusters and (1 1 1) γ-Al_2O_3 [23].

were rather large and thus prevented MoS_2 clusters from growing into large or layered clusters.

Sakashita [25] also studied the morphology and orientation of MoS_2 clusters on a (1 1 0) γ-Al_2O_3 thin film and an amorphous γ-Al_2O_3 substrate. For (1 1 0) γ-Al_2O_3, TEM photographs revealed no lattice image, but revealed blurry particles that were between 2 and 4 nm in diameter. These particles were assigned to thin MoS_2 layered clusters basal-bonded to the surface of γ-Al_2O_3. In fact, past studies pointed out that TEM observation could not detect small MoS_2 clusters [37,38] or thin MoS_2 layers [20,22] on γ-Al_2O_3 due to limited resolution of TEM between MoS_2 and Al_2O_3. For amorphous γ-Al_2O_3 surface, the TEM photograph showed numerous MoS_2 clusters with larger sizes than those observed on single-crystal surfaces, even when the sulfidation was done at a lower temperature.

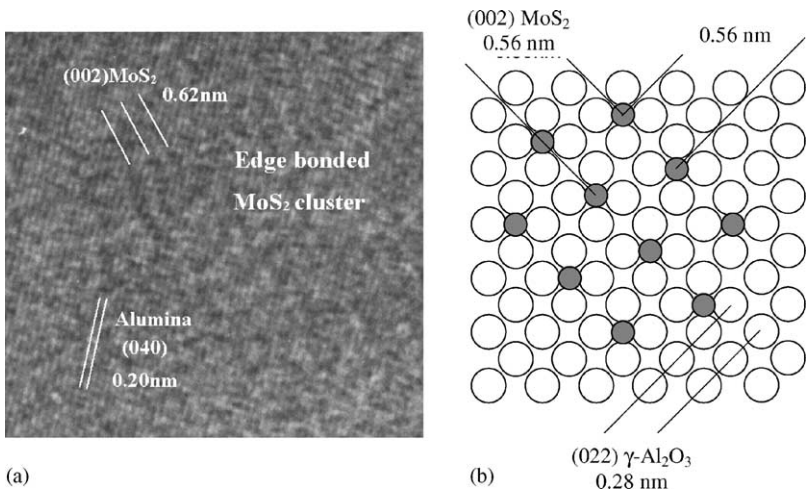

Fig. 6. (a) TEM photograph of MoS_2 clusters supported on (1 0 0) γ-Al_2O_3/$MgAl_2O_4$ substrate after sulfidation at 773 K and (b) schematic diagram of interface between MoS_2 clusters and (1 1 1) γ-Al_2O_3 [23].

Table 1
TEM observations of MoS_2 clusters on γ-Al_2O_3 thin film supports [25]

γ-Al_2O_3	Sulfided at 573 K[a]	Sulfided at 773 K[a]
(1 1 1)	No visible clusters	Basal, 1.7 nm, multi-layer, 9350/μm^2
(1 1 0)	No visible clusters	Basal, 2–4 nm, single-layer, N/A[b]
(1 0 0)	No visible clusters	Edge, 1.5 nm, 1.1 layer[c], 2400/μm^2
Amorphous γ-Al_2O_3 substrate	Edge + basal, 1.9 nm, 1.3 layer, 4208/μm^2	Edge + basal, 2.9 nm, 1.5 layer[c], 10098/μm^2

[a] Each column shows orientation, average length, stacking, and density of observed MoS_2 clusters.
[b] Could not be determined because particles were blurry in the image.
[c] Average numbers.

Table 1 summarizes the above TEM observation results for single-crystal surface and amorphous surface of γ-Al_2O_3 by Sakashita et al. [23–25]. Combining these results and XPS analytical results on the model catalysts before and after sulfidation, Sakashita [25] discussed the sulfidation behavior of MoO_x species on the surface. Before sulfidation, the dispersion increased in the order of (1 1 1) < (1 0 0) < (1 1 0). Sulfidation progressed most easily on (1 1 0) and most reluctantly on (1 1 1). These differences in dispersion and sulfidation order were attributed to the magnitude of the interaction between Mo species and γ-Al_2O_3 surface originating from the atomic arrangements at the interface; interaction between Mo species and γ-Al_2O_3 for (1 1 1) and (1 0 0) is relatively strong, whereas that between Mo species and (1 1 0) is relatively weak. Relatively well-grown MoS_2 clusters on amorphous γ-Al_2O_3 surface (Table 1) was attributed to the weak interaction between Mo species and γ-Al_2O_3 originating from the low density of surface hydroxyl groups [39]. In conclusion, the orientation of MoS_2 clusters on γ-Al_2O_3 surfaces was determined by the epitaxial relationship, in particular for (1 1 1) and (1 0 0) γ-Al_2O_3, where the interaction between MoS_2 clusters and the support surface is relatively strong.

3. Morphology and catalytic properties of MoS_2 clusters on γ-Al_2O_3 powder supports

The dependence of catalytic activities of MoS_2-based catalysts on the surface chemical properties of γ-Al_2O_3 powder supports has long been proposed. Ledoux et al. [40] investigated the effects of the Al_2O_3 phase on the HDS activity of Co–Mo catalysts. They reported that the HDS activity decreased in the order of γ- > η- > θ- > χ- > amorphous Al_2O_3, and concluded that this trend in the activity was not related to the microstructures of the Co–Mo catalysts but to the mean pore diameters of the Al_2O_3 supports. In contrast, Nishijima et al. [41] reported that the catalytic functions of γ-Al_2O_3 supported Mo catalysts, such as HYD and hydrocracking, differed among three kinds of γ-Al_2O_3 supports that were prepared by different methods yet had similar physical properties. They concluded that the different catalytic functions were due to the different morphologies of MoS_2 species (Fig. 2) that were affected by the chemical nature of each γ-Al_2O_3 support. Knozinger and Ratnasamy [36] reported that the chemical properties of the surface hydroxyl group on γ-Al_2O_3 depended on the surface microstructure and therefore differed on each crystal face.

The preceding section discussed results on the morphology and orientation of MoS_2 clusters on γ-Al_2O_3 single-crystal thin films. The remainder of this section discusses if those results can be applied to industrial catalysts supported on porous materials. The discussion will be extended to the catalytic activities of MoS_2 clusters with different morphologies supported on powder supports with different chemical nature.

Sakashita et al. [27] prepared MoS_2 catalysts supported on two kinds of γ-Al_2O_3 powder supports. One was plate-like (PL) γ-Al_2O_3 obtained by thermal treatment of commercially available boehmite, and the other was spherical (SP) γ-Al_2O_3 obtained by an evaporation technique. The PL Al_2O_3 powders with a parallelogram shape (Fig. 7a) exposed {1 1 1} planes as the side surfaces and {1 1 0} planes as the top and bottom surfaces (Fig. 7b). Note that ($h\,k\,l$), parenthesis, designate a *crystal face* or a *family of planes* throughout a crystal lattice, whereas {$h\,k\,l$},

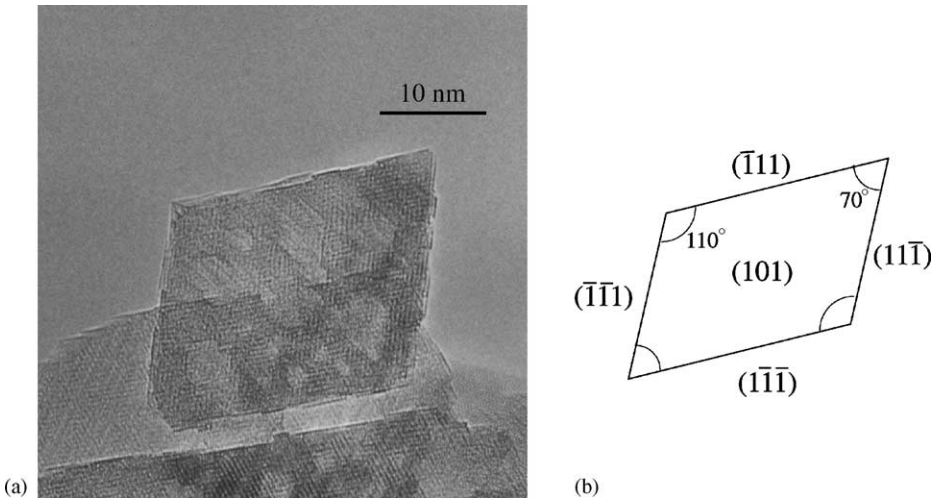

Fig. 7. (a) TEM photograph and (b) schematic diagram of PL γ-Al_2O_3 particle [27]. The faces with (1 1 1), ($\bar{1}$ 1 1), ($\bar{1}$ $\bar{1}$ 1), (1 1 $\bar{1}$), (1 $\bar{1}$ $\bar{1}$) belong to a set of crystal face, {1 1 1}. Similarly, the faces with (1 1 0) and (1 0 1) belong to the {1 1 0}-type set.

"squiggly" brackets, designate a set of faces that are equivalent by the symmetry of the crystal. The surface area ratio of {1 1 0} planes was about 80%, with the remainder surface area being {1 1 1} planes. This morphology only slightly differs from that of industrially prepared γ-Al_2O_3 from boehmite that has hexagonal PL shapes and exposes {1 1 0} planes as top and bottom surfaces and {1 1 1} and {1 0 0} surfaces as the side surfaces [39]. The SP powders (Fig. 8a) exposed mainly {1 1 1} and {1 0 0} planes (Fig. 8b). For a typical SP particle size of about 20 nm, the relative surface area ratios of {1 1 1} and {1 0 0} planes were similar, whereas for smaller particles the ratio of {1 1 1} planes became predominant.

The TEM photographs of the MoS_2 catalysts supported on PL and SP powders are shown in Fig. 9. For the PL powders (Fig. 9a), many single-layered MoS_2 clusters with lengths of 3–5 nm were observed

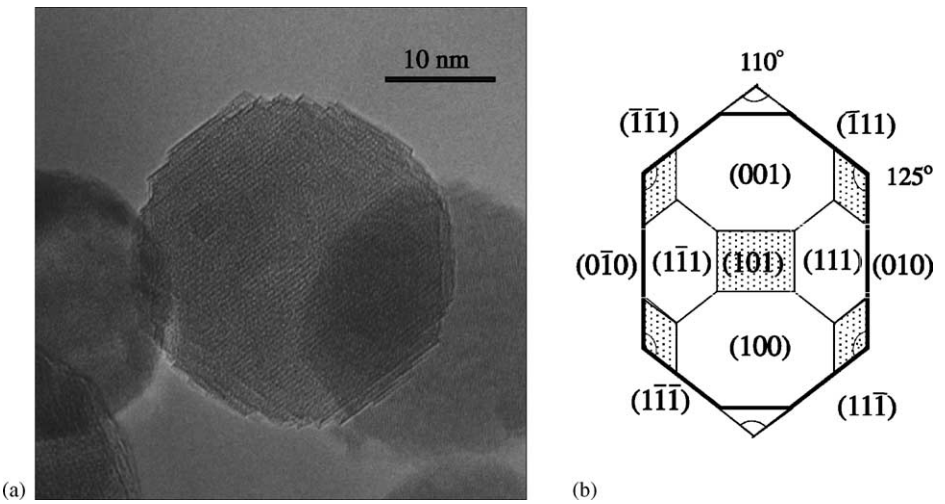

Fig. 8. (a) TEM photograph and (b) schematic of SP γ-Al_2O_3 particle [27]. The faces with (0 0 1) and (0 1 0) belong to the {1 0 0}-type set. The faces with dot-shading belong to the {1 1 0}-type set but consist of multiple {1 1 1} facets. Thus, {1 1 0}-type faces are not exposed.

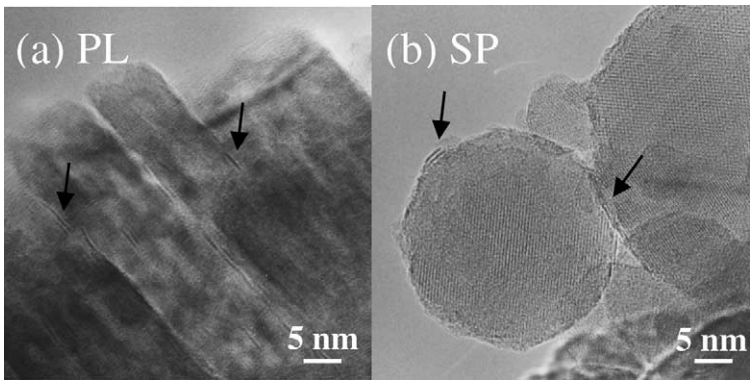

Fig. 9. TEM photographs of MoS_2 catalysts supported on γ-Al_2O_3 powders: (a) PL γ-Al_2O_3 (Mo loading of 4.2 wt.%) and (b) SP γ-Al_2O_3 (Mo loading of 3.1 wt.%). Catalysts (Mo loading of 4.6%) were prepared by equilibrium adsorption of ammonium heptamolybdate at pH = 2.0 and then calcined in nitrogen for 3 h at 773 K, followed by sulfidation by 5% H_2S/N_2 for 2 h at 673 K (arrows indicate MoS_2 clusters) [27].

at the interface of platelet-like crystals, indicating single-layered MoS_2 clusters basal-bonded to (1 1 0) planes. For the SP powders (Fig. 9b), although some stacked MoS_2 clusters (indicated by arrows in the figure) were observed, most of Mo species were assumed to be highly dispersed and not visible, because the density of the observed MoS_2 clusters was much smaller than that calculated from the Mo loading. These observations are consistent with the results on the morphology and orientation of MoS_2 clusters on γ-Al_2O_3 single-crystal faces summarized in Table 1; single-layered MoS_2 clusters were basal-bonded to the (1 1 0) planes of γ-Al_2O_3 powders. Relatively little information could be obtained for MoS_2 clusters on (1 0 0) and (1 1 1) planes, because MoS_2 clusters were visible only when the electron beam axis was identical to the [0 0 1] direction of the MoS_2 clusters or when the electron beam axis was perpendicular to the (0 0 1) plane of MoS_2 clusters with sufficient thickness [22].

Sakashita et al. [27] examined the catalytic activities of PL- and SP-supported MoS_2 catalysts by using two model test reactions, HYD of 1-methylnaphthalene (1-MN) and HDS of DBT. For both reactions, the SP-supported catalyst showed higher activities (Table 2). This superior activity of the SP-supported catalyst was attributed to the larger number of active catalytic sites on the SP γ-Al_2O_3, because the lateral size of MoS_2 clusters on the PL γ-Al_2O_3 was larger than that on the SP γ-Al_2O_3. The SP-supported catalyst was relatively HDS-oriented (Table 2). This was attributed to the higher stacking of MoS_2 clusters on the SP γ-Al_2O_3 with major surface planes of {1 1 1} and {1 0 0} than on the PL γ-Al_2O_3 that mainly exposes {1 1 0} planes, because MoS_2 clusters with low stacking were assumed to be HYD-oriented in both models proposed by Nishijima et al. [14] (Fig. 2) and Daage and Chianelli [18] (Fig. 3).

Table 2
Catalytic activities of MoS_2 supported catalysts on PL and SP γ-Al_2O_3 [27]

	HYD of 1-MN	HDS of DBT
MoS_2/PL, r_{SP}	0.66[a]	0.028[a]
MoS_2/SP, r_{PL}	0.97[a]	0.062[a]
Ratio (r_{SP}/r_{PL})	1.5	2.2

[a] Reaction rate, r (mol s^{-1} Mo^{-1}).

4. Morphology, orientation, and catalytic properties of MoS_2 clusters on TiO_2 powder supports

Edge-bonded MoS_2 clusters were observed on thin-film single-crystal model supports of γ-Al_2O_3, but were not confirmed on γ-Al_2O_3 powder supports. On a TiO_2 powder-supported MoS_2 catalyst, Sakashita et al. [28] obtained clear evidence for edge-bonded MoS_2 clusters by TEM observation. Fig. 10a shows a TEM photograph of MoS_2 clusters supported on

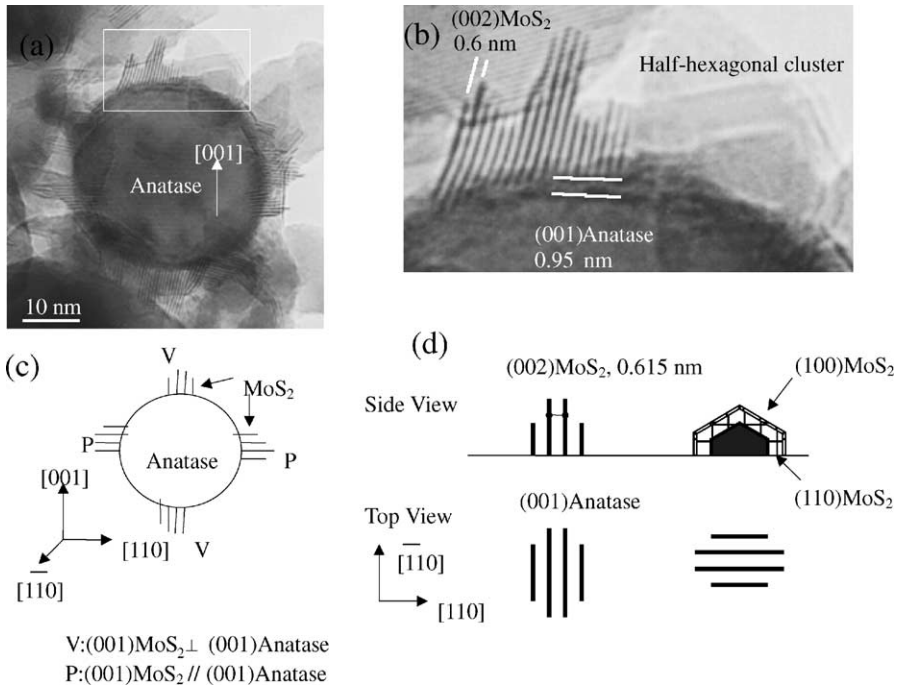

Fig. 10. (a, b) TEM photographs and (c, d) schematic diagrams of MoS_2 catalysts supported on TiO_2 powders. Catalysts (Mo loading of 4.6%) were prepared by equilibrium adsorption of ammonium heptamolybdate at pH = 2.0 and calcined in nitrogen for 3 h at 773 K, followed by sulfidation by 5% H_2S/N_2 for 2 h at 673 K [28].

ultrafine anatase-type TiO_2 particles with an average diameter of 30 nm. The line spacing of the stacked MoS_2 clusters was about 0.6 nm (Fig. 10b), identical to the (0 0 2) spacing of a MoS_2 crystal. Based on the 0.95 nm spacing of the horizontal planes of the TiO_2 support (Fig. 10b), which agreed with the (0 0 1) spacing of anatase, the orientation of spherical anatase particles was determined as shown in Fig. 10c. There were two different orientations; V:(0 0 1) $MoS_2 \perp$(0 0 1) anatase, and P:(0 0 1) MoS_2//(0 0 1) anatase. In addition to the stacked MoS_2 layers, half-hexagonal shaped structures were observed on the right side of Fig. 10b. These structures were assigned to MoS_2 clusters with peripheral (1 0 0) planes and formed with their (1 1 0) planes on (0 0 1) anatase as shown in Fig. 10d.

Fig. 11 shows a schematic diagram of the interface between (0 0 1) anatase and (1 1 0) MoS_2. The Ti–Ti distance along the [1 1 0] direction was 0.535 nm,

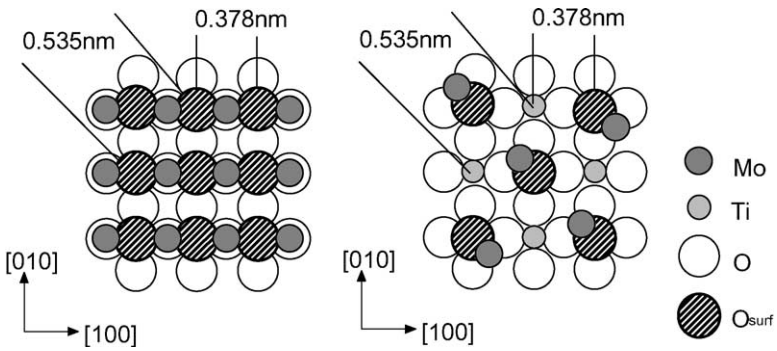

Fig. 11. Schematic diagram of the interface between (0 0 1) anatase and (1 1 0) MoS_2, assuming an Mo–O–Ti bond for each Mo atom.

which was only 2.2% smaller than the Mo–Mo distance of 0.547 nm in the (1 1 0) plane. This small misfit allowed the large MoS_2 clusters observed in Fig. 10a (17 layers with an average length of 7.2 nm). Similar to MoS_2 on γ-Al_2O_3, epitaxial relationships were observed between MoS_2 clusters and anatase surface planes. In contrast to the large lattice misfit (9%) between (1 0 0) γ-Al_2O_3 and MoS_2 clusters, the small lattice misfit (2%) between (0 0 1) anatase and MoS_2 clusters allowed the large edge-bonded layered MoS_2 clusters.

Subsequently, Araki et al. [29] studied the catalytic properties of edge-bonded MoS_2 catalysts. Fig. 12 shows TEM photographs of the MoS_2 catalysts calcined and sulfided under various conditions. When calcined in air and sulfided in H_2S/H_2 at 573 K, the catalysts (Fig. 12a) showed a small number of MoS_2 clusters as a monolayer or as bilayers. Because the Mo loading was 4.6%, the major part of the Mo species was not visible in the photograph due to high dispersion or insufficient sulfidation of Mo species. All the visible layers were parallel to the surface of TiO_2, namely, basal-bonded on the support. When sulfided in H_2S/N_2 at 573 K, the catalysts (Fig. 12b) showed many edge-bonded MoS_2 clusters with lengths shorter than 2 nm, although most of the MoS_2 clusters were not visible. With increasing sulfidation temperature, however, the edge-bonded clusters gradually changed their orientation into basal bonding (dotted circles in Fig. 12c and d) in addition to the growth of the edge-bonded

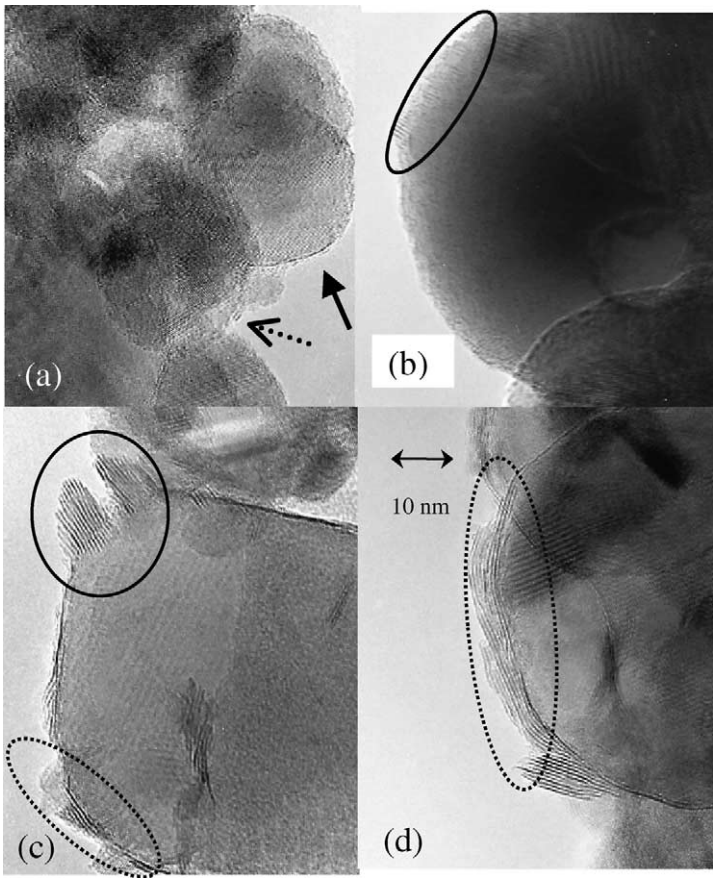

Fig. 12. TEM images of MoS_2 catalysts supported on TiO_2 powders. (a) Sulfided in H_2S/H_2 at 573 K, (b) sulfided in H_2S/N_2 at 573 K, (c) sulfided in H_2S/N_2 at 673 K, and (d) sulfided in H_2S/N_2 at 773 K. Catalysts were calcined in air. Solid arrow indicates a mono-layered basal-bonded MoS_2 cluster, dotted arrow indicates a two-layered MoS_2 cluster, solid circle indicates edge-bonded MoS_2 clusters, and dotted circle indicates basal-bonded MoS_2 clusters [29].

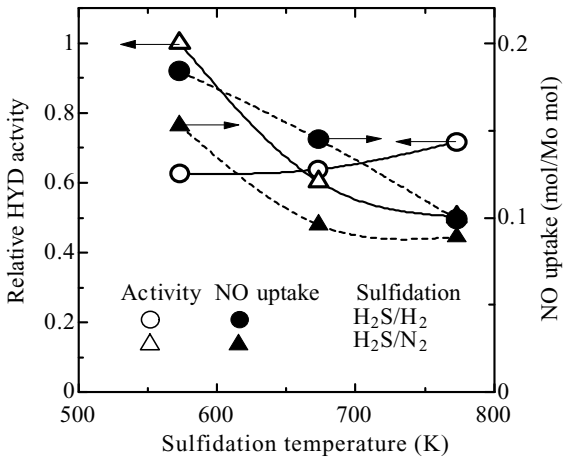

Fig. 13. Catalytic HYD activity and NO uptake of MoS_2/TiO_2 catalysts sulfided under different conditions [29]. The relative HYD activities were obtained by the HYD of 1-MN and calculated relative to that of the catalyst sulfided at 573 K in H_2S/N_2.

clusters (solid circle in Fig. 12c). Note that the effect of the calcination atmosphere on the orientation was relatively small, although the catalysts calcined in N_2 (Fig. 10a) showed larger MoS_2 clusters than those calcined in air (Fig. 12c). The genesis of edge-bonded MoS_2 clusters was reported related to the formation of MoS_3 [42–45] during sulfidation. Furthermore, sulfidation of the catalyst in H_2S/N_2 was reported likely to maintain the amorphous MoS_3 structures at higher temperature than does sulfidation in H_2S/H_2.

Araki et al. [29] measured the catalytic HYD activities and NO uptake over several MoS_2/TiO_2 catalysts sulfided under different conditions (Fig. 13). When sulfidation was done at 573 K, the HYD activity of the catalyst sulfided in H_2S/N_2 was higher than that of the catalyst sulfided in H_2S/H_2, although the NO uptake over the H_2S/N_2-sulfided catalyst was slightly lower than that over H_2S/H_2-sulfided catalyst. This was attributed to higher intrinsic activity of edge-bonded MoS_2 clusters than that of basal-bonded MoS_2 clusters. In fact, among all the catalysts investigated by Araki et al., the catalyst sulfided at 573 K in H_2S/N_2 showed the highest catalytic activity due to the high dispersion of the edge-bonded MoS_2 clusters with high intrinsic activity, although high temperature sulfidation caused serious aggregation of edge-bonded MoS_2 clusters and reduced the catalytic activities (Fig. 13). Based on the results of Fig. 13, Araki et al. also concluded that the intrinsic activities over catalysts sulfided in H_2S/N_2 were relatively independent of the dispersion, whereas the intrinsic activities of catalysts sulfided in H_2S/H_2 increased with decreasing dispersion. The increase in intrinsic activity was attributed to the increasing stacking of basal-bonded MoS_2 clusters that would result in the decrease in the electronic interaction between MoS_2 clusters and the TiO_2 support. Thus, the total activities of MoS_2 clusters shown in Fig. 4 increased in the following order: "MoS_2 clusters with edge-bonding" > "multi-layered MoS_2 clusters with basal-bonding" > "single-layered MoS_2 clusters with basal-bonding".

Many studies reported that the catalytic activities of TiO_2-supported MoS_2 catalysts were superior to those of Al_2O_3-supported catalysts [46–51]. Numerous discussions have been generated about possible reasons for this superiority. In most of those discussions, the superiority was attributed to differences in high dispersion [52,53] or high degree of sulfidation [50,54] caused by Mo–TiO_2 interaction. In contrast, some recent reports [55,56] attribute the superior activity of TiO_2-supported catalysts to a synergetic effect induced by partially reduced TiO_2, similar to the effect induced by Co or Ni. The results reported by Araki et al. [29] does not preclude the synergy effect of TiO_2, but have shown that the surface structure of TiO_2 facilitates the formation of edge-bonded MoS_2 clusters that can contribute to the high activity of TiO_2-supported catalysts.

5. Summary

Based on the results for γ-Al_2O_3 single-crystal thin films as model supports, the morphology and orientation of MoS_2 clusters depend on the surface atomic arrangements of γ-Al_2O_3 [23–25]. Namely, TEM observations showed that multi-layered MoS_2 clusters are basal-bonded to (1 1 1) γ-Al_2O_3 and that single-layered MoS_2 clusters are basal-bonded to (1 1 0) γ-Al_2O_3, whereas MoS_2 clusters are edge-bonded to (1 0 0) γ-Al_2O_3. The observation of edge-bonded MoS_2 clusters differed from previous TEM observations [20,22] that showed no edge-bonded MoS_2 clusters on various oxide supports. One possible reason for this difference is that edge-bonded MoS_2 clusters on γ-Al_2O_3 were easily overlooked because the sizes of edge-bonded MoS_2 clusters were limited

due to the large lattice misfit between MoS_2 clusters and (1 0 0) γ-Al_2O_3. Relatively large edge-bonded MoS_2 clusters with high stacking were observed on the anatase-type TiO_2 powders [28]. This high stacking was attributed to the small misfit between MoS_2 clusters and (0 0 1) anatase.

The relationship between the morphology and orientation and the catalytic activities have been investigated for MoS_2 catalysts supported on γ-Al_2O_3 [27] and TiO_2 [29] powders. The results obtained for γ-Al_2O_3 powders were consistent with the rim-edge model [18], in which MoS_2 clusters with low stacking were HYD-oriented and those with high stacking were HDS-oriented. Results for TiO_2-supported catalysts show that multi-layered MoS_2 clusters possess higher intrinsic activities than single-layered MoS_2 clusters. This result is consistent with the comparison between Co–Mo–S(I) and Co–Mo–S(II) [4]; multi-layered Co–Mo–S(II) has higher intrinsic activity due to smaller electronic interaction with the catalyst support than do single-layered Co–Mo–S(I). Furthermore, the intrinsic activity of edge-bonded MoS_2 clusters was found to be superior to that of basal-bonded MoS_2 clusters in the HYD reaction [29]. High temperature sulfidation was found to change the orientation of edge-bonded MoS_2 clusters to basal-bonding. Further studies are needed to determine how to stabilize the edge-bonded MoS_2 clusters to the support.

References

[1] M. Houalla, D. Broderick, V.J.H. de Beer, B.C. Gates, H. Kwart, Prepr. Am. Chem. Soc., Div. Petroleum Chem. 22 (1977) 941.
[2] S.S. Katti, D.W.B. Westerman, B.C. Gates, T. Youngless, L. Petrakis, Ind. Eng. Chem., Process Des. Dev. 23 (1984) 773.
[3] T. Kabe, A. Ishihara, Q. Zang, Appl. Catal. A 97 (1993) L1.
[4] H. Topsøe, B.S. Clausen, R. Candia, C. Wivel, S. Mørup, J. Catal. 68 (1981) 433.
[5] H. Topsøe, B.S. Clausen, F.E. Massoth, Hydrotreating catalysis, in: J.R. Anderson, M. Boudart (Eds.), Catalysis Science and Technology, vol. 11, Springer, Berlin, 1996.
[6] R. Candia, O. Sørensen, J. Villadsen, N.-Y. Topsøe, B.S. Clausen, H. Topsøe, Bull. Soc. Chim. Belg. 93 (1984) 763.
[7] S.M.A.M. Bouwens, F.B.M. van Zon, M.P. van Dijk, A.M. van der Kraan, V.H.J. de Beer, J.A.R. van Veen, D.C. Koningsberger, J. Catal. 146 (1994) 375.
[8] H. Topsøe, B.S. Clausen, N.-Y. Topsøe, P. Zeuthen, Stud. Surf. Sci. Catal. 53 (1990) 77.
[9] J. Ramirez, S. Fuentes, G. Diaz, M. Vrinat, M. Breysse, M. Lacroix, Appl. Catal. 52 (1989) 211.
[10] S. Eijsbouts, Appl. Catal. A 158 (1997) 53.
[11] V.M. Brown, S.P.A. Louwers, R. Prins, Catal. Today 10 (1991) 345.
[12] S.P.A. Louwers, M.W.J. Craje, A.M. van der Kraan, C. Geantet, R. Prins, J. Catal. 144 (1993) 579.
[13] D.D. Whitehurst, T. Isoda, I. Mochida, Adv. Catal. 42 (1998) 345.
[14] A. Nishijima, H. Shimada, T. Sato, Y. Yoshimura, N. Matsubayashi, T. Kameoka, J. Jpn. Petrol. Inst. (Sekiyu Gakkaishi) 32 (1989) 35 (in Japanese).
[15] M. Vrinat, M. Breysse, C. Geantet, J. Ramirez, F.E. Massoth, Catal. Lett. 26 (1994) 25.
[16] F.E. Massoth, G. Muralidhar, in: Proceedings of the Fourth International Conference on the Chemistry and Uses of Molybdenum, Climax Molybdenum Co., 1982, p. 343.
[17] S. Kasztelan, L. Jalowiecki, A. Wambeke, J. Grimblot, J.P. Bonnelle, Bull. Soc. Chim. Belg. 96 (1987) 1003.
[18] M. Daage, R.R. Chianelli, J. Catal. 149 (1994) 414.
[19] K.C. Pratt, J.V. Sanders, V. Christov, J. Catal. 124 (1990) 416.
[20] S. Srinivasan, A.K. Datye, C.H.F. Peden, J. Catal. 137 (1992) 513.
[21] T.F. Hayden, J.A. Dumesic, J. Catal. 103 (1987) 366.
[22] R.M. Stockmann, H.W. Zandbergen, A.D. van Langeveld, J.A. Moulijn, J. Mol. Catal. A 102 (1995) 147.
[23] Y. Sakashita, T. Yoneda, J. Catal. 185 (1999) 487.
[24] Y. Sakashita, N. Aoki, T. Yoneda, Stud. Surf. Sci. Tech. Catal. 121 (1998) 403.
[25] Y. Sakashita, Surf. Sci. 489 (2001) 45.
[26] Y. Sakashita, Y. Araki, K. Honna, H. Shimada, in: Proceedings of the 12th International Congress on Catalysis, 1998.
[27] Y. Sakashita, Y. Araki, H. Shimada, Appl. Catal. A 215 (2001) 101.
[28] Y. Sakashita, Y. Araki, K. Honna, H. Shimada, Appl. Catal. A 197 (2000) 247.
[29] Y. Araki, K. Honna, H. Shimada, J. Catal. 207 (2002) 361.
[30] G.C.A. Schuit, B.C. Gates, AIChE J. 19 (1973) 417.
[31] N.S. Mcintyre, T.C. Chan, P.A. Spevack, Appl. Catal. 63 (1990) 391.
[32] E. Diemann, Th. Weber, A. Muller, J. Catal. 148 (1994) 288.
[33] J.C. Muijsers, Th. Weber, R.M. van Hardeveld, H.W. Zandbergen, J.W. Niemantsverdriet, J. Catal. 157 (1995) 698.
[34] A.M. De Jong, V.H.J. de Beer, J.A.R. van Veen, J.W. Niemantsverdriet, J. Vac. Sci. Tech. A 15 (1997) 1592.
[35] K. Josek, Ch. Linsmeier, H. Knozinger, E. Taglauer, Nucl. Instr. Meth. Phys. Res. B 64 (1992) 596.
[36] H. Knozinger, P. Ratnasamy, Catal. Rev.-Sci. Eng. 17 (1978) 31.
[37] M.J. Yacaman, C. Zorrilla, J.A. Ascencio, G. Mondragon, J. Reyes-Gasga, Mater. Trans. JIM 40 (1999) 141.
[38] S. Eijsbouts, J.J.L. Heinerman, Appl. Catal. A 105 (1993) 53.
[39] P. Nortier, P. Fourre, Appl. Catal. 61 (1990) 141.
[40] M. Ledoux, A. Peter, E.A. Blekkan, F. Luck, Appl. Catal. A 133 (1995) 321.
[41] A. Nishijima, H. Shimada, T. Sato, Y. Futamura, N. Matsubayashi, T. Kameoka, J. Jpn. Petrol. Inst. (Sekiyu Gakkaishi) 31 (1988) 109.
[42] Th. Weber, J.C. Muijsers, J.W. Niemantsverdriet, J. Phys. Chem. 99 (1995) 9194.

[43] J.C. Muijsers, Th. Weber, R.M. van Hardeveld, H.W. Zandbergen, J.W. Niemantsverdriet, J. Catal. 157 (1995) 698.
[44] E. Payen, S. Kasztelan, S. Houssenbay, R. Szymanski, J. Grimblot, J. Phys. Chem. 93 (1989) 6501.
[45] M. de Boer, A.J. van Dillen, D.C. Koningsberger, J.W. Geus, J. Phys. Chem. 98 (1994) 7862.
[46] S. Matsuda, A. Kato, Appl. Catal. 8 (1983) 149.
[47] K.Y.S. Ng, E. Gulari, J. Catal. 95 (1985) 33.
[48] H. Shimada, T. Sato, Y. Yoshimura, J. Hiraishi, A. Nishijima, J. Catal. 110 (1988) 275.
[49] J. Ramirez, S. Fuentes, G. Diaz, M. Vrinat, M. Breysse, M. Lacroix, Appl. Catal. 52 (1989) 211.
[50] Y. Okamoto, A. Maezawa, T. Imanaka, J. Catal. 120 (1989) 29.
[51] F. Luck, Bull. Chim. Soc. Belg. 100 (1991) 781.
[52] J. Ramirez, L. Ruiz-Ramirez, L. Cedeno, V. Hale, M. Vrinat, M. Breysse, Appl. Catal. A 93 (1993) 163.
[53] R.G. Leliveld, A.J. van Dillen, J.W. Geus, D.C. Koningsberger, J. Catal. 171 (1997) 115.
[54] S. Yoshinaka, K. Segawa, Catal. Today 45 (1998) 293.
[55] J. Ramirez, L. Cedeno, G. Busca, J. Catal. 184 (1999) 59.
[56] L. Coulier, J.A.R. van Veen, J.W. Niemantsverdriet, Catal. Lett. 79 (2002) 149.